# Mass Outflow Rate From Advective Accretion Disks around Compact Objects

Tapas K. Das and Sandip K. Chakrabarti S.N. Bose National Centre for Basic Sciences, JD Block, Salt Lake, Sector-III, Calcutta-700091 e-mail: tdas@boson.bose.res.in & chakraba@boson.bose.res.in

# **ABSTRACT**

We compute mass outflow rates from advective accretion disks around compact objects, such as neutron stars and black holes. These computations, for the first time, are done using combinations of exact transonic inflow and outflow solutions which may or may not form standing shock waves. Assuming that the bulk of the outflow is from the effective boundary layers of these objects, we find that the ratio of the outflow rate and inflow rate varies anywhere from a few percent to even close to a hundred percent (i.e., close to disk evacuation case) depending on the initial parameters of the disk, the degree of compression of matter near the centrifugal barrier, and the polytropic index of the flow. Our result, in general, matches with the outflow rates obtained through a fully time-dependent numerical simulation. In some region of the parameter space when the standing shock does not form, our results *indicate* that the disk may be evacuated and may produce quiescence states.

Subject headings: black holes — neutron stars— stars: accretion — stars:winds — shocks waves — jets — AGN — quasars

Submitted to ApJ in April 1998; Still trying to teach the referee the meaning of centrifugal barrier and the funnel wall.

## 1. Introduction

One of the signatures of activities around compact objects is the presence of jets and outflows. Outflows carry away angular momentum from the accretion disk and are partially responsible for the accretion itself. Active galaxies and quasars are supposed to harbor black holes at their centers and at the same time produce cosmic radio jets through

which immense amount of matter and energy are ejected out of the core of the galaxies (See, Begelman, Blandford & Rees, 1984 and Chakrabarti, 1996a for reviews). Similarly, micro-quasars have also been discovered very recently where outflows are formed from stellar black hole candidates (Mirabel & Rodriguez, 1994). Many of these outflows show superluminal motions which are probably due to magnetic effects. With hydrodynamic effects alone, which we are employing in this paper, one should not be able to accelerate the flow more than the initial sound velocity. A well known stellar object SS433 (which is believed to be a neutron star), where pure hydrodynamic effects may be operating, produces outflows with a speed roughly one-third of the speed of light.

There are several models in the literature which study the origin, formation and collimation of these outflows. Difference between stellar outflows and outflows from these systems is that the outflows in these systems have to form out of the inflowing material only. This is because black holes and neutron stars have no atmospheres of their own. The models present in the literature are roughly of three types. The first type of solutions confine themselves to the jet properties only, completely decoupled from the internal properties of accretion disks. They study the effects of hydrodynamic or magneto-hydrodynamic pressures on the origin of jets (e.g., Blandford & Payne 1982; Ferrari et al., 1985; Fukue 1987; Contopoulus 1985; Chakrabarti, 1990). In the second type, efforts are made to correlate the internal disk structure with that of the outflow using both hydrodynamic (e.g., Chakrabarti 1986) and magnetohydrodynamic considerations (Königl 1989; Chakrabarti & Bhaskaran 1992). In the third type, numerical simulations are carried out to actually see how matter is deflected from the equatorial plane towards the axis (e.g., Hawley, Smarr & Wilson, 1984; Eggum, Katz & Coroniti, 1985; Molteni, Lanzafame & Chakrabarti, 1994; Molteni, Ryu & Chakrabarti, 1996; Ryu, Chakrabarti & Molteni, 1997). From the analytical front, although the wind type solutions and accretion type solutions come out of the same set of governing equations (Chakrabarti 1990), there were no attempt to find connections among them. As a result, the estimation of the outflow rate from the inflow rate has always been impossible. On the other hand, the mass outflow rate of the normal stars are calculated very accurately from the stellar luminosity. Theory of radiatively driven winds seems to be very well understood (e.g., Castor, Abott & Klein, 1975). The simplicity of black holes and neutron stars lie in the fact that they do not have atmospheres. But the disks surrounding them have, and similar method as employed in stellar atmospheres should be applicable to the disks. Our approach in this paper is precisely this. We first determine the properties of the rotating inflow and outflow and identify solutions to connect them. In this manner we self-consistently determine the mass outflow rates.

Before we present our results, we describe basic properties of the rotating inflow and outflow. A rotating inflow with a specific angular momentum  $\lambda(x)$  entering into a black

hole will have angular momentum  $\lambda \sim \text{constant}$  close to the black hole for any moderate viscous stress. This is because the viscous time scale is generally much longer compared to the infall time scale and even though at the outer edges the angular momentum distribution may be Keplerian or even super-Keplerian matter would be highly sub-Keplerian close to the black hole. This is because the flow has to enter through the horizon with velocity of light and presence of this large inertial (ram) force, in addition to usual gravitational and centrifugal forces, makes the flow sub-Keplerian. Almost constant angular momentum produces a very strong centrifugal force  $\lambda^2/x^3$  which increases much faster compared to the gravitational force  $\sim GM/x^2$  and becomes comparable at around  $x \sim l^2/GM$ , or,  $r_{cb} \sim 2\lambda^2$  where r and  $\lambda$  are x and l, written in units of  $R_q = 2GM/c^2$  and  $R_q c = 2GM/c$ respectively. The subscript cb under r stands for the centrifugal barrier. (In the rest of the paper, we use  $R_g$  as the length unit, c is the unit of velocity, and the mass of the black hole M to the unit of mass.) Here, (actually, a little farther out, due to thermal pressure) matter starts piling up and produces the centrifugal pressure supported boundary layer (CENBOL). Further close to the black hole, the gravity always wins and matter enters the horizon supersonically after passing through a sonic point. CENBOL may or may not have a sharp boundary, depending on whether standing shocks form or not. Generally speaking, in a polytropic flow, if the polytropic index  $\gamma > 1.5$ , then shocks do not form and if  $\gamma < 1.5$ , only a region of the parameter space forms the shock (C96b). In any case, the CENBOL forms. In this region the flow becomes hotter and denser and for all practical purposes behaves as the stellar atmosphere so far as the formation of outflows are concerned. Inflows on neutron stars behave similarly, except that the 'hard-surface' inner boundary condition dictates that the flow remain subsonic between the CENBOL and the surface rather than becoming supersonic as in the case of a black hole. In case where the shock does not form, regions around pressure maximum achieved just outside the inner sonic point would also drive the flow outwards. In the back of our mind, we have the picture of the outflow as obtained by Hawley, Smarr & Wilson (1984), Chakrabarti (1986) and Molteni, Ryu and Chakrabarti (1996), namely, that the outflow is thermally and centrifugally accelerated but confined by external pressure of the ambient medium.

There are two surfaces of utmost importance in flows with angular momentum. One is the 'funnel wall' where the effective potential (sum of gravitational potential and the specific rotational energy) vanishes. In the case of a purely rotating flow, this is the 'zero pressure' surface. Flows *cannot* enter inside the funnel wall because the pressure would be negative. The other surface is called the 'centrifugal barrier'. This is the surface where the radial pressure gradient of a purely rotating flow vanishes and is located *outside* the funnel wall simply because the flow pressure is higher than zero on this surface. Flow with inertial pressure easily crosses this 'barrier' and either enters into a black hole or flows out

as winds depending on its initial parameters (detail classification of the parameter space is in Chakrabarti, 1989) In numerical simulations (e.g., Hawley, Smarr & Wilson, 1984; Molteni, Ryu and Chakrabarti, 1996) it is observed that the outflow generally hugs the 'funnel wall' and goes out in between these two surfaces. In this paper we assume precisely this. However, we believe that the cross section area could be weakly influenced by the pressence of the small outward radial motion of the flow. We have ignored such a correction.

Outflow rates from accretion disks around black hole and neutron stars must be related to the properties of CENBOL which in turn, depend on the inflow parameters. Subsonic outflows originating from CENBOL would pass through sonic points and reach far distances as in wind solutions. Assuming free-falling conical polytropic inflow and isothermal outflows (as in stellar winds), it is easy to estimate the ratio of outflowing and inflowing rates (Chakrabarti, 1997a; 1998):

$$\frac{\dot{M}_{out}}{\dot{M}_{in}} = R_{in} = \frac{\Theta_{out}}{\Theta_{in}} \frac{R}{4} e^{-(f_0 - \frac{3}{2})} f_0^{3/2}$$

where,  $\Theta_{out}$  and  $\Theta_{in}$  are the solid angles of the outflow and inflow respectively, and

$$f_0 = \frac{(2n+1)R}{2n}.$$

Here, R is the compression ratio of inflowing matter at the CENBOL and  $n=1/(\gamma-1)$  is the polytropic constant. When  $\Theta_{out} \sim \Theta_{in}$ ,  $R_{\dot{m}} \sim 0.052$  and 0.266 for  $\gamma=4/3$  and 5/3 respectively. Assuming a thin inflow and outflow of  $10^o$  conical angle, the ratio  $R_{\dot{m}}$  becomes 0.0045 and 0.023 respectively.

The aim of the present paper is to compute the mass loss rate more realistically than what has been attempted so far. We calculate this rate as a function of the inflow parameters, such as specific energy and angular momentum, accretion rate, polytropic index etc. We explore both the polytropic and the isothermal outflows. Our conclusions show that the outflow rate is sensitive to the specific energy and accretion rate of the inflow. Specifically, when the outflow is not isothermal, outflow rate generally increases with the specific energy and the polytropic index  $\gamma_o$  of the outflow, generally decreases with the polytropic index  $\gamma$  of the inflow, but somewhat insensitive to the specific angular momentum  $\lambda$ . In the case of isothermal outflow, however, mass loss rate is sensitive to the inflow rate, since the inflow rate decides the proton temperature of the advective region of the disk which in turn fixes the outflow temperature. In this case the outflow is at least partially temperature driven. The outflow rate is also found to be anti-correlated with specific angular momentum  $\lambda$  of the flow.

The plan of this paper is the following: In the next Section, we describe our model and present the governing equations for the inflow and outflow. In §3, we present the solution

procedure of the equations. In §4, we present results of our computations. Finally, in §5, we draw our conclusions.

# 2. Model Description and Governing Equations

### 2.1. Inflow Model

For the sake of computation of the inflow quantities, we assume that the inflow is axisymmetric and thin: h(r) << r, so that the transverse velocity component could be ignored compared to the radial and azimuthal velocity components. We consider polytropic inflows in vertical equilibrium (otherwise known as 1.5 dimensional flows, see, Chakrabarti, 1989; hereafter referred to as C89). We ignore the self-gravity of the flow and viscosity is assumed to be significant only at the shock, if present. We do the calculations using Paczyński-Wiita (1980) potential which mimics surroundings of the Schwarzschild black hole. The equations (in dimensionless units) governing the inflow are:

(a) Conservation of specific energy is given by,

$$\mathcal{E} = \frac{u_e^2}{2} + na_e^2 + \frac{\lambda^2}{2r^2} - \frac{1}{2(r-1)}.$$
 (1)

where,  $u_e$  and  $a_e$  are the radial and polytropic sound velocities respectively.  $a_e = (\gamma p_e/\rho_e)^{1/2}$ ,  $p_e$  and  $\rho_e$  are the pressure and density of the flow. For a polytropic flow,  $p_e = K \rho_e^{\gamma}$ , where K is a constant and is a measure of entropy of the flow. Here,  $\lambda$  is the specific angular momentum and n is the polytropic constant of the inflow  $n = (\gamma - 1)^{-1}$ ,  $\gamma$  is the polytropic index. The subscript e refers that the quantities are measured on the equatorial plane.

Mass conservation equation, apart from a geometric constant, is given by,

$$\dot{M}_{in} = u_e \rho_e r h_e(r), \tag{2}$$

where  $h_e(r)$  is the half-thickness of the flow at radial co-ordinate r having the following expression

$$h_e(r) = a_e r^{\frac{1}{2}} (r-1) \sqrt{\frac{2}{\gamma}}.$$
 (3a)

Another useful way of writing the mass inflow is to introduce an entropy dependent quantity  $\dot{\mathcal{M}} \propto \gamma^n K^n \dot{M}$  which can be expressed as

$$\dot{\mathcal{M}} = u_e a_e^{\alpha} r^{\frac{3}{2}} (r - 1) \sqrt{\frac{2}{\gamma}} \tag{3b}$$

Where,  $\dot{\mathcal{M}}$  is really the entropy accretion rate (C89). When the shock is not present,  $\dot{\mathcal{M}}$  remains constant in a polytropic flow. When the shock is present,  $\dot{\mathcal{M}}$  will increase at the shock due to increase of entropy.  $\alpha = (\gamma + 1)/(\gamma - 1) = 2n + 1$ . If the centrifugal pressure supported shock is present, the usual Rankine-Hugoniot conditions, namely, conservations of mass, energy and momentum fluxes across the shock are to be taken into account (C89) in determining the shock locations. In presence of mass loss one must incorporate this effect in the shock condition (see, eq. 15 below).

#### 2.2. Outflow Models

We consider two types of outflows. In ordinary stellar mass loss computations (e.g. Tarafdar, 1988, and references therein), the outflow is assumed to be isothermal till the sonic point. This assumption is probably justified, since copious photons from the stellar atmosphere deposit momenta on the slowly outgoing and expanding outflow and possibly make the flow close to isothermal. This need not be the case for outflows from compact sources. Centrifugal pressure supported boundary layers close to the black hole are very hot (close to the virial temperature) and most of the photons emitted may be swallowed by the black holes themselves instead of coming out of the region and depositing momentum onto the outflow. Thus, the outflows could be cooler than isothermal flows. In our first model, we choose polytropic outflows with same energy as the inflow (i.e., no energy dissipation between the inflow and outflow) but with a different polytropic index  $\gamma_o < \gamma$ . Nevertheless, it may be advisable to study the isothermal outflow to find out the behavior of the extreme case. Thus an isothermal outflow is chosen in our second model. In each case, of course, we include the possibility that the *inflow* may or may not have standing shocks.

It is to be noted that we chose the outflows to be propagating through the funnel wall even though the inflow is assumed to be thin. This may not be completely self-inconsistent. On the one hand, our assumption of thin inflow is for the sake of computation of the thermodynamic quantities only, but the flow itself need not be physically thin. Secondly, the funnel wall and the centrifugal barrier are purely geometric surfaces, and they exist anyway and the outflow could be supported even by ambient medium which may not necessarily be a part of the disk itself. So, we believe that our assumptions are not entirely unjustified.

# 2.2.1. Polytropic Outflow

In this case, the energy conservation equation takes the form:

$$\mathcal{E} = \frac{\vartheta^2}{2} + n'a_e^2 + \frac{\lambda^2}{2r_m^2(r)} - \frac{1}{2(r-1)}$$
(4)

and the mass conservation in the outflow takes the form:

$$\dot{M}_{out} = \rho \vartheta \mathcal{A}(r). \tag{5}$$

Here,  $n' = (\gamma_o - 1)^{-1}$  is the polytropic constant of the outflow. The difference between eq. (4) and eq. (1) is that, presently, the rotational energy term contains

$$r_m(r) = \frac{\Re(r) + R(r)}{2},\tag{6a}$$

as the mean *axial* distance of the flow. The expression of  $\Re(r)$ , the local radius of the centrifugal barrier comes from balancing the centrifugal force with the gravity (Molteni, Ryu & Chakrabarti, 1996), i.e.,

$$\frac{\lambda^2}{\Re^3(r)} = \frac{\Re(r)}{2r(r-1)^2}.$$
 (6b)

We thus obtain,

$$\Re(r) = \left[2\lambda^2 r(r-1)^2\right]^{\frac{1}{4}} \tag{7a}$$

And the expression for R(r), the local radius of the funnel wall, comes from vanishing of total effective potential, i.e.,

$$\Omega_{toteff}(r) = -\frac{1}{2(r-1)} + \frac{\lambda^2}{2R^2(r)} = 0$$

$$R(r) = \lambda \left[ (r-1) \right]^{1/2}$$
(7b)

The difference between eq. (5) and eq. (2) is that the area functions are different. Here, A(r) is the area between the centrifugal barrier and the funnel wall (see introduction for the motivation). This is computed with the assumption that the outflow is external pressure supported, i.e., the centrifugal barrier is in pressure balanced with the ambient medium. Matter, if pushed hard enough, can cross centrifugal barrier in black hole accretion (the reason why rapidly rotating matter can enter into a black hole in the first place). An outward thermal force (such as provided by the CENBOL) in between the funnel wall and the centrifugal barrier causes the flow to come out. Thus the cross section of the outflow is,

$$\mathcal{A}(r) = \pi[\Re^2(r) - R^2(r)]. \tag{8}$$

The outflow angular momentum  $\lambda$  is chosen to be the same as in the inflow, i.e., no viscous dissipation is assumed to be present in the inner region of the flow close to a black hole. Considering that viscous time scales are longer compared to the inflow time scale, it may be a good assumption in the disk, but it may not be a very good assumption for the outflows which are slow prior to the acceleration and are therefore, prone to viscous transport of angular momentum. Such detailed study has not been attempted here particularly because we know very little about the viscous processes taking place in the pre-jet flow. Therefore, we concentrate only those cases where the specific angular momentum is roughly constant when inflowing matter becomes part of the outflow, although some estimates of the change in  $R_m$  is provided when the average angular momentum of the outflow is lower. Detailed study of the outflow rates in presence of viscosity and magnetic field is in progress and would be presented elsewhere.

# 2.2.2. Isothermal Outflow

The integration of the radial momentum equation yields an equation similar to the energy equation (eq. 4):

$$\frac{\vartheta_{iso}^{2}}{2} + C_{s}^{2} ln\rho + \frac{\lambda^{2}}{2r_{m}(r)^{2}} - \frac{1}{2(r-1)} = \text{Constant}$$
 (9)

In this case the thermal energy term is different, behaving logarithmically. The constant sound speed of the outflow is  $C_s$ . The mass conservation equation remains the same:

$$\dot{M}_{out} = \rho \vartheta_{iso} \mathcal{A}(r). \tag{10}$$

Here, the area function remains the same above. A subscript *iso* of velocity  $\vartheta$  is kept to distinguish from the velocity in polytropic case. This is to indicate the velocities are measured here using completely different assumptions.

In both the models of the outflow, we assume that the flow is primarily radial. Thus the  $\theta$ -component of the velocity is ignored ( $\vartheta_{\theta} << \vartheta$ ).

# 3. Procedure to solve for disks and outflows simultaneously

Before we go into the details, a general understanding of the transonic flows around a black hole is essential. In Chakrabarti (1989, 1996c), all the solution topologies of the polytropic flow in pseudo-Newtonian geometry has been provided (e.g., see, Fig. 3)

Chakrabarti, 1996c) In regions I and O of the parameter space the flow has only one sonic point. Matter with positive energy at a large distance must pass through that point before entering into the black hole supersonically. In regions SA and SW shocks may form in accretion and winds respectively, but no shocks are expected in winds and accretions if parameters are chosen from these branches. In NSW and NSA, two saddle type sonic points exist, but no steady shock solutions are possible.

Suppose that matter first enters through the outer sonic point and passes through a shock. At the shock, part of the incoming matter, having higher entropy density is likely to return back as winds through a sonic point, other than the one it just entered. Thus a combination of topologies, one from the region **SA** and the other from the region **O** is required to obtain a full solution. In the absence of the shocks, the flow is likely to bounce back at the pressure maximum of the inflow and since the outflow would be heated by photons, and thus have a smaller polytropic constant, the flow would leave the system through an outer sonic point different from that of the incoming solution. Thus finding a complete self-consistent solution boils down to finding the outer sonic point of the outflow and the mass flux through it. Below we present the list of parameters used in both of our models and briefly describe the procedure to obtain a satisfactory solution.

# 3.1. Polytropic Outflow

We assume that

- (a) In this case, a very little amount of total energy is assumed to be lost in each bundle of matter as it leaves the disk and joins the jet. The specific energy  $\mathcal{E}$  remains fixed throughout the flow trajectory as it moves from the disk to the jet.
- (b) Very little viscosity is present in the flow except at the place where the shock forms, so that the specific angular momentum  $\lambda$  is constant in both inflows and outflows close to the black hole. At the shock, entropy is generated and hence the outflow is of higher entropy for the same specific energy.
- (c) The polytropic index of the inflow  $(\gamma)$  and outflow  $(\gamma_o)$  are free parameters and in general,  $\gamma_o < \gamma$ , because of heating effect of the outflow (e.g., due to the momentum deposition coming out of the disk surface). In reality  $\gamma_o$  is directly related to the heating and cooling processes of the outflow. When  $\dot{M}_{in}$  is high, heating of outflow by photon momentum deposition is higher, and therefore  $\gamma_o \to 1$ .

Thus a supply of parameters  $\mathcal{E}$ ,  $\lambda$ ,  $\gamma$  and  $\gamma_o$  make a self-consistent computation of  $R_m$  possible when the shock is present. When the shock is absent, the compression ratio of the

gas at the pressure maximum between the inflow and outflow  $R_{comp}$  is supplied as a free parameter, since it may be otherwise very difficult to compute satisfactorily. In the presence of shocks, such problems do not arise as the compression ratio is obtained self-consistently.

The following procedure is adopted to obtain a complete solution:

(a) From eqs. (1) and (2) we derive an expression for the derivative,

$$\frac{du}{dr} = \frac{\frac{\lambda^2}{r^3} + \frac{na^2}{\alpha} + \frac{5r - 3}{r(r - 1)} - \frac{1}{2(r - 1)^2}}{u - \frac{2na^2}{\alpha u}}.$$
 (11)

At the sonic point, the numerator and denominator separately vanish, and give rise to the so-called sonic point conditions:

$$a_{c} = \frac{\frac{1}{2(r_{c}-1)^{2}} - \frac{\lambda^{2}}{r_{c}^{3}}}{\frac{\alpha(r_{c}-1)r_{c}}{n(5r_{c}-3)}}$$
(12a)

$$u_c = \sqrt{\frac{2n}{\alpha}} a_c \tag{12b}$$

where, the subscript c represents the quantities at the sonic point. The derivative of the flow at the sonic point is computed using the L'Hospital's rule. Using fourth order Runge-Kutta method  $\vartheta(r)$  and a(r) are computed along the flow till the position where the Rankine-Hugoniot condition is satisfied (if shocks form) and from there on the sub-sonic branch is integrated for the accretion as usual (C89). With the known  $\gamma_o$ ,  $\mathcal{E}$  and  $\lambda$ , one can compute the location of the outflow sonic point from eqs. (4) and (5),

$$\frac{d\vartheta}{dr} = \frac{\frac{a^2}{\mathcal{A}^2(r)} \frac{d\mathcal{A}(r)}{dr} + \frac{\lambda^2}{r_m^3(r)} \frac{dr_m(r)}{dr} - \frac{1}{2(r-1)^2}}{\vartheta - \frac{a^2}{\vartheta}}$$
(13)

from where the sonic point conditions at the outflow sonic point  $r_{co}$  obtained are given by,

$$\frac{a_{co}^2}{\mathcal{A}_{co}^2(r)} \frac{d\mathcal{A}(r)}{dr} \Big|_{co} + \frac{\lambda^2}{r_{mco}^3(r)} \frac{dr_m(r)}{dr} \Big|_{co} - \frac{1}{2(r_{co} - 1)^2} = 0$$
 (14a)

and

$$\vartheta_{co} = a_{co}. (14b)$$

At the outer sonic point, the derivative of  $\vartheta$  is computed using the L'Hospital's rule and the Runge-Kutta method is used to integrate towards the black hole to compute the velocity of the outflow at the shock location. The density of the outflow at the shock is computed by distributing the post-shock dense matter of the disk into spherical shell of  $4\pi$  solid angle. The outflow rate is then computed using eq. (5).

It is to be noted that when the outflows are produced, one cannot use the usual Rankine-Hugoniot relations at the shock location, since mass flux is no longer conserved *in accretion*, but part of it is lost in the outflow. Accordingly, we use,

$$\dot{M}_{+} = (1 - R_{\dot{m}})\dot{M}_{-} \tag{15}$$

where, the subscripts + and - denote the pre- and post-shock values respectively. Since due to the loss of matter in the post-shock region, the post-shock pressure goes down, the shock recedes backward for the same value of incoming energy, angular momentum & polytropic index. The combination of three changes, namely, the increase in the cross-sectional area of the outflow and the launching velocity of the outflow and the decrease in the post-shock density decides whether the net outflow rate would increased or decreased than from the case when the exact Rankine-Hugoniot relation was used.

In the case where the shocks do not form, the procedure is a bit different. It is assumed that the maximum amount of matter comes out from the place of the disk where the thermal pressure of the inflow attains its maximum. The expression for the polytropic pressure for the inflow in vertical equilibrium is,

$$\mathcal{P}_e(r) = \frac{a_e^{2(n+1)} \dot{M}_{in}}{\gamma^{(1+n)} \dot{\mathcal{M}}} \tag{16}$$

This is maximized and the outflow is assumed to have the same quasi-conical shape with annular cross-section  $\mathcal{A}(r)$  between the funnel wall and the centrifugal barrier as already defined. In the absence of shocks the compression ratio of the flow between the incoming flow and outgoing flow at the pressure maximum cannot be computed self-consistently unlike the case when the shock was present. Thus this ratio is chosen freely. We take the guidance for this number from what was obtained in the case when shocks are formed. However, in this case even when the mass loss takes place, the location of the pressure maximum remains unchanged. Since the compression ratio  $R_{comp}$  is a free parameter,  $R_{\dot{m}}$  remains unchanged for a given  $R_{comp}$ . Let us assume that  $\dot{\mu}_-$  is the actual mass inflow rate and it is same before and after the pressure maximum had the mass loss rate been negligible. Let  $\dot{\mu}_+$  be the mass inflow rate after the pressure maximum, when the loss due to outflow is taken into account. Then, by definition,  $\dot{\mu}_- = \dot{M}_{out} + \dot{\mu}_+$  and  $R_{\dot{m}} = \dot{M}_{out}/\dot{\mu}_-$ .

Thus the *actual* ratio of the mass outflow rate and the mass inflow rate, when the mass loss is taken into consideration is given by,

$$\frac{\dot{M}_{out}}{\dot{\mu}_{+}} = \frac{R_{\dot{m}}}{1 - R_{\dot{m}}}.\tag{17a}$$

However, this static consideration is valid only when  $R_{\dot{m}} < 1$ . Otherwise, we must have,

$$-\frac{dM_{disk}}{dt} + \dot{\mu}_{-} = \dot{\mu}_{+} + \dot{M}_{out}$$

i.e.,

$$-\frac{dM_{disk}}{dt} = \dot{\mu}_{-}(R_{\dot{m}} - 1) + \dot{\mu}_{+} \tag{17b}$$

Here,  $M_{disk}$  is the instantaneous mass of the disk. Since  $R_m > 1$ , the disk has to evacuate. These cases hint that the assumptions of the steady solution breaks down completely and the solutions may become become highly time dependent.

#### 3.2. Isothermal Outflow

We assume that

- (a) The outflow has exactly the *same* temperature as that of the post-shock flow, but the energy is not conserved as matter goes from disk to the jet. In other words the outflow is kept in a thermal bath of temperature as that of the post-shock flow.
- (b) Same as (b) of §3.1.
- (c) The post-shock proton temperature is determined from the inflow accretion rate  $M_{in}$  using the consideration of Comptonization of the advective region. The procedure to compute typical proton temperature as a function of the incoming accretion rate has been adopted from Chakrabarti (1997b).
- (d) The polytropic index of the inflow can be varied but that of the outflow is always unity.

Thus a supply of parameters  $\mathcal{E}$ ,  $\lambda$  and  $\gamma$  makes a self-consistent computation of  $R_m$  possible when the shock is present. When the shock is absent, the compression ratio of the gas at the pressure maximum between the inflow and the outflow  $R_{comp}$  is supplied as a free parameter exactly as in the polytropic case.

The following procedure is adopted to obtain a complete solution:

(a) From eqs. (9) and (10) we derive an expression for the derivative,

$$\frac{d\vartheta}{dr}|_{iso} = \frac{\frac{C_s^2}{\mathcal{A}(r)} \frac{d\mathcal{A}(r)}{dr} + \frac{\lambda^2}{r_m^3(r)} \frac{dr_m(r)}{dr} - \frac{1}{2(r_c - 1)^2}}{\vartheta_{iso} - \frac{C_s^2}{\vartheta_{iso}}}.$$
(18)

At the sonic point, the numerator and denominator separately vanish, and give rise to the so-called sonic point conditions:

$$\frac{C_s^2}{\mathcal{A}_{co}(r)} \frac{d\mathcal{A}(r)}{dr} \Big|_{co} + \frac{\lambda^2}{r_{m_{co}}^3(r)} \frac{dr_m(r)}{dr} \Big|_{co} - \frac{1}{2(r_{co} - 1)^2} = 0, \tag{19a}$$

and

$$\vartheta_{co} = C_s, \tag{19b}$$

where, the subscript co represents the quantities at the sonic point of the outflow. The derivative of the flow at the sonic point is computed using the L'Hospital's rule. The procedure is otherwise similar to those mentioned in the polytropic case and we do not repeat them here.

# 4. Results

## 4.1. Polytropic outflow coming from the post-shock accretion disk

Figure 1 shows a typical solution which combines the accretion and the outflow. The input parameters are  $\mathcal{E}=0.0005$ ,  $\lambda=1.75$  and  $\gamma=4/3$  corresponding to relativistic inflow. The solid curve with an arrow represents the pre-shock region of the inflow and the long-dashed curve represents the post-shock inflow which enters the black hole after passing through the inner sonic point (I). The solid vertical line at  $X_{s3}$  (the leftmost vertical transition) with double arrow represents the shock transition obtained with exact Rankine-Hugoniot condition (i.e., with no mass loss). The actual shock location obtained with modified Rankine-Hugoniot condition (eq. 15) is farther out from the original location  $X_{s3}$ . Three vertical lines connected with the corresponding dotted curves represent three outflow solutions for the parameters  $\gamma_o = 1.3$  (top), 1.15 (middle) and 1.05 (bottom). The outflow branches shown pass through the corresponding sonic points. It is evident from the figure that the outflow moves along solution curves completely different from that of the 'wind solution' of the inflow which passes through the outer sonic point 'O'. The mass loss ratio  $R_{\hat{m}}$  in these cases are 0.256, 0.159 and 0.085 respectively. Figure 2 shows the ratio  $R_{\hat{m}}$  as  $\gamma_o$  is varied. Only the range of  $\gamma_o$  and energy for which the shock-solution is present

is shown here. The general conclusion is that as  $\gamma_o$  is increased the ratio is also increased non-linearly. When the inflow rate is very low, due to paucity of the photons, the outflow is not heated very much and  $\gamma_o$  remains higher. The reverse is true when the accretion rate is higher. Thus, effectively, the ratio  $R_m$  is going up with the decrease in  $\dot{M}_{in}$ . In passing we remark that with the variation in the inflow angular momentum,  $\lambda$ , the result does not change significantly, and  $R_m$  changes only by a couple of percentage at the most.

In Fig. 3a, we show the variation of the ratio  $R_m$  of the mass outflow rate and inflow rate as a function of the shock-strength (dotted)  $M_{-}/M_{+}$  (Here,  $M_{-}$  and  $M_{+}$  are the Mach numbers of the pre- and post-shock flows respectively.), the compression ratio (solid)  $\Sigma_{+}/\Sigma_{-}$  (Here,  $\Sigma_{-}$  and  $\Sigma_{+}$  are the vertically integrated matter densities in the pre- and post- shock flows respectively), and the stable shock location (dashed)  $X_{s3}$  (in the notation of C89). Other parameters are  $\lambda = 1.75$  and  $\gamma_o = 1.05$ . Note that the ratio  $R_m$  does not peak near the strongest shocks! Shocks are stronger when they are located closer to the black hole, i.e., for smaller energies. It is interesting to note that the general shape of  $R_m$ variation roughly agrees with analytical results of Chakrabarti (1997a; 1998) where it was shown that for a finite outflow compression ratio must be non-zero and  $R_m$  peaks at an intermediate compression ratio. The non-monotonic behavior is more clearly seen in lowest curve of Fig. 3b where  $R_m$  is plotted as a function of the specific energy  $\mathcal{E}$  (along x-axis) and  $\gamma_o$  (marked on each curve). Specific angular momentum is chosen to be  $\lambda = 1.75$ as before. The tendency of the peak in  $R_m$  is primarily because as  $\mathcal{E}$  is increased, the shock location is increased which generally increases the outflowing area  $\mathcal{A}(r)$  at the shock location. However, the density of the outflow at the shock, as well as the velocity of the outflow at the shock increases. The outflow rate, which is a product of these quantities, thus shows a peak. For the sake of comparison, we present the results for  $\gamma_o = 1.05$  (dashed curve) when the Rankine-Hugoniot relation was not corrected by eq. (15). The result generally remains the same because of two competing effects: decrease in post-shock density and increase in the area from the the outflow is launched (i.e., area between the black hole and the shock) as well as the launching velocity of the jet at the shock.

To have a better insight of the behavior of the outflow we plot in Fig. 4  $R_m$  as a function of the polytropic index of the *incoming* flow ( $\gamma$ ) for  $\gamma_o = 1.1$ ,  $\mathcal{E} = 0.002$  and  $\lambda = 1.75$ . The range of  $\gamma$  shown is the range for which shock forms in the flow. We also plot the variation of injection velocity  $\vartheta_{inj}$ , injection density  $\rho_{inj}$  and area  $\mathcal{A}(r)$  of the outflow at the location where the outflow leaves the disk. The incoming accretion rate has been chosen to be 0.3 (in units of the Eddington rate). These quantities are scaled from the corresponding dimensionless quantities as  $\vartheta_{inj} \to 0.1\vartheta_{inj}$ ,  $\rho_{inj} \to 10^{22}\rho_{inj}$  and  $\mathcal{A} \to 10^{-4}\mathcal{A}$  respectively in order to bring them in the same scale. With the increase in  $\gamma$ , the shock location is increased, and therefore the cross-sectional area of the outflow goes up. The

injection velocity goes up (albeit very slowly) as the shock recedes, since the injection surface (CENBOL) comes closer to the outflow sonic point. However, the density goes down (gas is less denser). This anti-correlation is reflected in the peak of  $R_{\dot{m}}$ .

So far, we assumed that the specific angular momentum of the outflow is exactly the same as that of the inflow, while in reality it could be different due to presence of viscosity. In the outflow, a major source of viscosity is the radiative viscosity whose coefficient is,

$$\eta = \frac{4aT^4}{15\kappa_T c\rho} \text{ cm}^2 \text{ sec}^{-1} \tag{20}$$

This could be significant, since the temperature of the outflow is high, but the density is low. Assuming that the angular momentum distribution reaches a steady state inside the jet (Chakrabarti, 1986 and references therein),

$$l_i = C_i R^{n_j} \tag{21}$$

where  $C_j$  and  $n_j$  are constants, the vanishing condition of the azimuthal velocity on the axis requires that  $n_j > 1$  inside the jet. The matter distribution in the rotationally dominant region of the 'pre-jet' is computed by integrating Euler equation. It is easy to show that the 'hollow' jet thus produced carry most of the matter and angular momentum in the outer layers of the jet (Chakrabarti, 1986). In other words, the average angular momentum of the outflow away from the base may remain roughly constant even in presence of viscosity. This is to be contrasted with the disk, where matter is more dense towards the centre while more angular momentum is concentrated towards the outer edge. If, however, the average angular momentum at the base of the outflow goes does down due to losses to ambient medium, by, say, a factor of two, we find that the mass loss rate is also reduced by around the same factor. This shows that the outflow is at least partially centrifugally driven.

An important point to note: the ratio between the 'specific entropy measure' of the outflow to that of the post-shock inflow is obtained from the definitions of entropy accretion rate  $\dot{\mathcal{M}}$  (see, eq. 3b):

$$\frac{K_o}{K_+} = \frac{\dot{\mathcal{M}}_{out}^{\gamma_o - 1}}{\dot{\mathcal{M}}_+^{\gamma_o - 1}} \left(\frac{1 - R_{\dot{m}}}{R_{\dot{m}}}\right)^{\gamma_o - 1} \dot{M}_+^{(\gamma_o - \gamma_o)} \frac{\gamma}{\gamma_o}$$

$$\tag{22}$$

As  $R_{\dot{m}} \to 1$ ,  $\frac{K_o}{K_+} \to 0$ . Thus, we expect that for a polytropic flow with shocks, a hundred percent outflow is impossible since the outgoing entropy must be higher. In isothermal outflows such simple consideration do not apply.

If we introduce an extra radiation pressure term (with a term like  $\Gamma/r^2$  in the radial force equation, where  $\Gamma$  is the contribution due to radiative process), particularly important for neutron stars, the outcome is significant. In the inflow, outward radiation pressure

weakens gravity and thus the shock is located farther out. The temperature is cooler and therefore the outflow rate is lower. If the term is introduced only in the outflow, the effect is not significant.

# 4.2. Polytropic outflow coming from the region of the maximum pressure

In this case, the inflow parameters are chosen from region I (see C96c) so that the shocks do not form. Here, the inflow passes through the inner sonic point only. The outflow is assumed to be originated from the regions where the polytropic inflow has a maximum pressure. This assumption is justified, since it is expected that winds would get the maximum kick at this region. Figure 5a shows a typical solution. The arrowed solid curve shows the inflow and the dotted arrowed curves show the outflows for  $\gamma_o = 1.3$  (top), 1.1 (middle) and 1.01 (bottom). The ratio  $R_m$  in these cases is given by 0.66, 0.30 and 0.09 respectively. The specific energy and angular momentum are chosen to be  $\mathcal{E} = 0.00584$  and  $\lambda = 1.8145$  respectively. The pressure maximum occurs outside the inner sonic point at  $r_p$ when the flow is still subsonic. Figure 5b shows the variation of thermal pressure of the flow with radial distance. The peak is clearly visible. Since the pressure maximum occurs very close to the black hole as compared to the location of the shock, the area of the outflow is smaller, but the radial velocity as well as the density of matter at the base of the outflow are much higher. As a result the outflow rate is exorbitantly higher compared to the shock case. Figure 6 shows the ratio  $R_m$  as a function of  $\gamma_o$  for various choices of the compression ratio  $R_{comp}$  of the outflowing gas at the pressure maximum:  $R_{comp} = 2$  for the rightmost curve and 7 for the leftmost curve. We have purposely removed the solutions with  $R_m > 1$ , because the solution should be inherently time-dependent (see, eq. 17b) in these cases and a steady state approach is not supposed to be trusted completely. This is different from the results of §4.1, where shocks are considered, since  $R_{\dot{m}}$  is non-monotonic in that case. It is also found that in some range of parameters, the very high massflow could take place even for smaller compression ratios especially when the sonic point of the outflow  $r_o$  is right outside the pressure maximum. These cases can cause runaway instabilities by rapidly evacuating the disk. They may be responsible for quiescent states in X-ray novae systems and also in some systems with massive black holes (e.g., our own galactic centre?), although it is not clear if such a phase of profuse mass loss has been directly observed.

The location of maximum pressure being close to the black hole, it may be generally very difficult to generate the outflow from this region. Thus, it is expected that the ratio  $R_{\dot{m}}$  would be larger when the maximum pressure is located farther out. This is exactly what we see in Fig. 7, where we plot  $R_{\dot{m}}$  against the location of the pressure maximum

(solid curve). Secondly, if our guess that the outflow rate could be related to the pressure is correct, then the rate should increase as the pressure at the maximum rises. That is also observed in Fig. 7. We plot here  $R_{\dot{m}}$  as a function of the actual pressure at the pressure maximum (dotted curve). The mass loss is found to be a strongly correlated with the thermal pressure. Here we have multiplied non-dimensional thermal pressure by  $1.5 \times 10^{24}$  in order to bring it in the same scale.

# 4.3. Isothermal outflow coming from the post-shock accretion disk

In this case, the outflow is assumed to be isothermal. The temperature of the outflow is obtained from the proton temperature of the advective region of the disk. The proton temperature is obtained using the Comptonization, bremsstrahlung, inverse bremsstrahlung and Coulomb processes (Chakrabarti, 1997b and references therein). Figure 8 shows the effective proton temperature and the electron temperature of the post-shock advective region as a function of the accretion rate (in units of Eddington rate, in logarithmic scale) of the Keplerian component of the disk. The diagram is drawn for a black hole of mass  $10M_{\odot}$ . The soft X-ray luminosity for stellar mass black holes or the UV luminosity of massive black holes is basically dictated by the Keplerian rate of the disk. It is clear that as the accretion rate of the Keplerian disk is increased, the advective region gets cooler as is expected.

In Fig. 9a, we show the ratio  $R_m$  as a function of the accretion rate (in units of Eddington rate) of the incoming flow for a range of the specific angular momentum. In the low luminosity objects the ratio is larger. Angular momentum is varied from  $\lambda=1.7$  (top curve), 1.725 (middle curve) and 1.75 (bottom curve). The specific energy is  $\mathcal{E}=0.003$ . Here we have used the modified Rankine-Hugoniot relation as before (eq. 15). The ratio  $R_m$  is clearly very sensitive to the angular momentum since it changes the shock location rapidly and therefore changes the post-shock temperature very much. We also plot the outflux of angular momentum  $F(\lambda)=\lambda\dot{m}_{in}R_m$  which has a maximum at intermediate accretion rates. In dimensional units, these quantities represent significant fractions of angular momentum of the entire disk and therefore the rotating outflow can help accretion processes. Curves are drawn for different  $\lambda$  as above. In Fig. 9b, we plot the variation of the ratio directly with the proton temperature of the advecting region. The outflow is clearly thermally driven. Hotter flow produces more winds as is expected. The angular momentum associated with each curve is same as before.

# 4.4. Isothermal outflow coming from the region of the maximum pressure

This case produces very similar result as in the above case, except that like Section 4.2 the outflow rate becomes very close to a hundred percent of the inflow rate when the proton temperature is very high. Thus, when the accretion rate of the Keplerian flow is very small, the outflow rate becomes very high, close to evacuating the disk. As noted before, this may also be related to the quiescent state of the X-ray novae.

## 5. Conclusions

In this paper, we have computed the mass outflow rate from the advective accretion disks around galactic and extra-galactic black holes. Since the general physics of advective flows are similar around a neutron star, we believe that the conclusions may remain roughly similar provided the shock at  $X_{s3}$  forms, although the boundary layer (which corresponds to  $X_{s1}$  in C89 notation; also see C96b) of the neutron star, where half of the binding energy could be released, may be more luminous than that of a black hole and may thus affect the outflow rate. We have chosen a limited number of free parameters just sufficient to describe the inflow and only one extra parameter for the outflow. We find that the outflow rates can vary from a very few percentage of the inflow rate, to as much as the inflow rate (causing almost complete evacuation of the accretion disk) depending on the inflow parameters. For the first time, it became possible to use the exact transonic solutions for both the disks and the winds and combine them to form a self-consistent disk-outflow system. Although we present results when centrifugally supported boundary layers are considered around a black hole, it is evident that the result is general, namely, if such a barrier is produced by other means, such as pre-heating (Chang & Ostriker, 1985) or by pair-plasma pressure (Kazanas & Ellison, 1986), outflows would also be produced (Das, in preparation).

The basic conclusions of this paper are the followings:

- a) It is possible that most of the outflows are coming from the centrifugally supported boundary layer (CENBOL) of the accretion disks.
- b) The outflow rate generally increases with the proton temperature of CENBOL. In other words, winds are, at least partially, thermally driven. This is reflected more strongly when the outflow is isothermal.
- c) Even though specific angular momentum of the flow increases the size of the CENBOL, and one would have expected a higher mass flux in the wind, we find that the rate of the outflow is actually anti-correlated with the  $\lambda$  of the inflow. On the other hand, if the

angular momentum of the outflow is reduced by hand, we find that the rate of the outflow is correlated with  $\lambda$  of the outflow. This suggests that the outflow is partially centrifugally driven as well.

- d) The ratio  $R_{\dot{m}}$  is generally anti-correlated with the inflow accretion rate. That is, disks of lower luminosity would produce higher  $R_{\dot{m}}$ .
- e) Generally speaking, supersonic region of the inflow do not have pressure maxima. Thus, outflows emerge from the subsonic region of the inflow, whether the shock actually forms or not.

In this paper, we assumed that the magnetic field is absent. Centrifugally driven winds (e.g., Blandford & Payne, 1982), electromagnetically accelerated winds (Lovelace, 1976; Lovelace, Wang & Sulkanen, 1987; Contopoulos & Lovelace, 1994 etc.) and winds from Blandford & Znajek (1977) process have not been considered here. These effects have so far been considered in the context of a Keplerian disk and *not* in the context of sub-Keplerian flows on which we concentrate here. Secondly, whereas the entire Keplerian disk was assumed to participate in wind formation, here we suggest that CENBOL is the major source of outflowing matter. It is not unreasonable to assume that CENBOL would still form when magnetic fields are present (Chakrabarti, 1990) and since the Alfvén speed is, by definition, higher compared to the sound speed, the acceleration, and therefore the mass outflow would also be higher than what we computed here. Such works would be carried out in future.

In the literature, not many results are present which deal with exact computations of the mass outflow rate. Molteni, Lanzafame & Chakrabarti (1994), in their SPH simulations, found that the ratio could be as high as 15-20 per cent when the flow is steady. In Ryu, Chakrabarti & Molteni (1997), 10-15 per cent of the steady outflow is seen and occasionally, even 150 of the inflow is found to be ejected in non-stationary cases. Our result shows that high outflow rate is also possible, especially for absence of shocks and low luminosities. In Eggum, Coroniti & Katz (1985), radiation dominated flows showed  $R_m \sim 0.004$ , which also agrees with our results when we consider high accretion rates (see, e.g., Fig. 9a). Observationally, it is very difficult to obtain the outflow rate from a real system, as it depends on too many uncertainties, such as filling factors and projection effects. In any case, with a general knowledge of the outflow rate, we can now proceed to estimate several important quantities. For example, it had been argued that the composition of the disk changes due to nucleosynthesis in accretion disks around black holes and this modified isotopes are deposited in the surroundings by outflows from the disks (Hogan & Applegate 1987; Mukhopadhyay & Chakrabarti, 1998 and references therein). Similarly, it is argued that outflows deposit magnetic flux tubes from accretion disks into the surroundings (Daly & Loeb, 1990). Thus a knowledge of outflows are essential in understanding varied physical phenomena in galactic environments.

A number of possible improvements could be made on this basic work. For instance, the effect of radiation pressure on both the inflows and outflows are to be taken into account self-consistently, particularly when the neutron star winds are considered. A preliminary investigation with a  $\Gamma/r^2$  force term (whose effect is to weaken gravity) suggests that for non-zero  $\Gamma$  in the inflow, the mass-loss rate changes significantly. This is because the shock location increases when  $\Gamma$  is increased. This in turn reduces the mass loss rate. On the other hand, the when  $\Gamma$  is non-zero in the outflow, the effect is not very high, since the outflow rate is generally driven by thermal effect of the *disk* and not the wind. Similarly, we see a significant reduction of the outflow when the average specific angular momentum of the outflow is reduced. This is expected since the outflow is partially centrifugally driven. This effect is stronger when the outflow is isothermal.

An interesting situation arises when the polytropic index of the outflow is large and the compression ratio of the flow is also very high. In this case, the flow virtually bounces back as the winds and the outflow rate can be equal to the inflow rate or even higher, thereby evacuating the disk. In this range of parameters, most, if not all, of our assumptions may breakdown completely because the situation could become inherently time-dependent. It is possible that some of the black hole systems, including that in our own galactic centre, may have undergone such evacuation phase in the past and gone into quiescent phase.

So far, we made the computations around a Schwarzschild black hole. In the case of a Kerr black hole (C96c), the shock locations will come closer and the outflow rates should become higher. Similarly magnetic field will change the sonic point locations significantly (C90). The mass outflow rates in these conditions are being studied and the results would be reported elsewhere (Das, 1998b). We made a few assumptions, some of which may be questionable. Our assumption of the wind formation from the post-shock region is very similar to the assumptions involved in computing mass outflow rate from stellar atmospheres. This is because the post-shock region behaves like a boundary layer. However, when the shocks are not formed, we assumed that the outflow comes out of the region of maximum pressure. Whereas, this may be a plausible assumption, it is not clear if strong outflows actually form from that close to the black hole. Similarly, whereas the assumption of isothermality in the stellar system may be justified, it is questionable if this can be rigorously valid in the present system since the proton temperatures are too high, and to maintain that high temperature till the sonic point, the disk has to deposit enormous energy into the winds. Nevertheless, we believe that our calculation is sufficiently illustrative and gives a direction which can be followed in the future for further refinements.

We thank the unknown referee for his helpful suggestions.

#### REFERENCES

Begelman, M.C., Blandford, R.D. & Rees, M.J. 1984, Rev. Mod. Phys., 56, 255

Blandford, R. D. & Payne, D. 1982, MNRAS, 199, 883

Castor, J. I., Abott, D. C. & Klein, R. I. 1975, ApJ, 195, 157

Chakrabarti, S. K. 1986, ApJ, 303, 582

Chakrabarti, S. K. 1989, ApJ, 347, 365 (C89)

Chakrabarti, S. K. 1990, Theory of Transonic Astrophysical Flows (Singapore: World Sci.) (C90)

Chakrabarti, S. K. 1996a, in Accretion Processes on Black Holes, Physics Reports, v. 266, No. 5 & 6, p 229 (C96a)

Chakrabarti, S. K. 1996b, ApJ, 464, 664 (C96b)

Chakrabarti, S. K. 1996c, MNRAS, 471, 237

Chakrabarti, S.K., 1997a, ApJ, submitted

Chakrabarti, S. K. 1997b, ApJ, 484, 313

Chakrabarti, S. K. 1998, in Observational Evidence for Black Holes in the Universe, Ed. S.K. Chakrabarti (Kluwer Academic: Holland), p. 19, (also in astro-ph/9807104)

Chakrabarti, S. K. & Bhaskaran, P. 1992, 255, 255

Chakrabarti, S. K., & Titarchuk, L.G. 1995, ApJ, 455, 623 (CT95)

Chang, K.M. & Ostriker, J.P. 1985, ApJ, 288, 428

Contopoulos, J. 1995, ApJ, 446, 67

Contopoulos, J. & Lovelace, R.V.E., 1994, ApJ, 429, 139.

Daly, R.A. & Loeb, A. 1990, ApJ, 364, 451

Das, T.K., 1998a, in Observational Evidence for Black Holes in the Universe, Ed. S.K. Chakrabarti (Kluwer Academic: Holland), p. 113, (also in astro-ph/9807105)

Das, T.K., 1998b, in preparation.

Eggum, G.E., Coroniti, F.V., Katz, J.I. 1985, ApJ, 298, L41

Ferrari, A. Trussoni, E., Rosner, R. & Tsinganos, K. 1985, ApJ, 294, 397

Fukue, J. 1982, PASJ, 34, 163

Hawley, J.W., Smarr, L. & Wilson, J. 1984, ApJ, 297, 296.

Hawley, J.F., Smarr, L.L., & Wilson, J.R. 1985, ApJS, 55, 211

Kazanas, D. & Ellison, D. C. 1986, ApJ304, 178.

Königl, A. 1989, ApJ, 342, 208

Lovelace, R.V.E. 1976, Nature, 262, 649

Lovelace, R.V.F., Wang J.C.L. & Sulkanen, M.E., 1987, ApJ 315, 504.

Margon, B. 1984, ARAA, 22, 507

Mirabel, I.F. & Rodriguez, L. F. 1994, Nat, 371, 46

Molteni, D., Sponholz, H. & Chakrabarti, S.K. 1996 ApJ, 457, 805

Molteni, D., Lanzafame, G. & Chakrabarti, S.K. 1994 ApJ, 425, 161

Molteni, D., Ryu., D. & Chakrabarti 1996, ApJ, 470, 460

Mukhopadhyay, B. & Chakrabarti, S.K., 1998, ApJ, submitted

Ryu, D., Chakrabarti, S.K., & Molteni, D. 1997, ApJ, 474, 378

Shapiro, S.L. 1973 ApJ, 180, 531

Tarafdar, S.P. 1988, ApJ, 331, 932

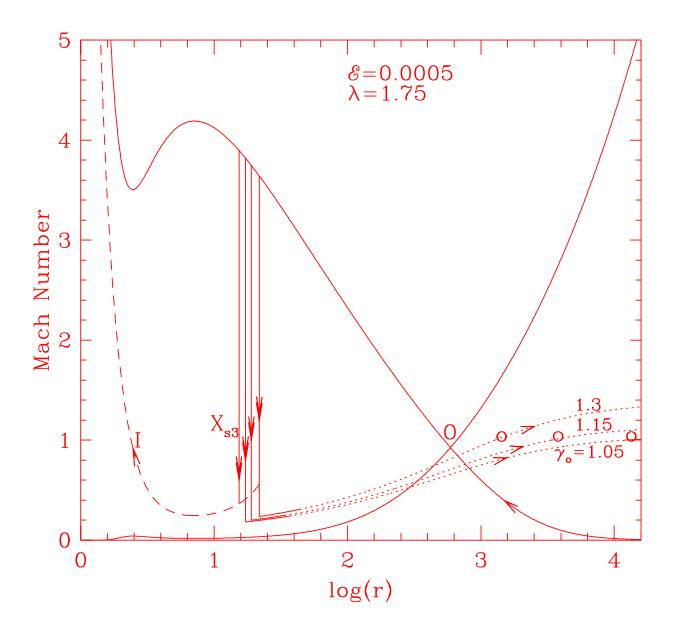
This preprint was prepared with the AAS IATEX macros v4.0.

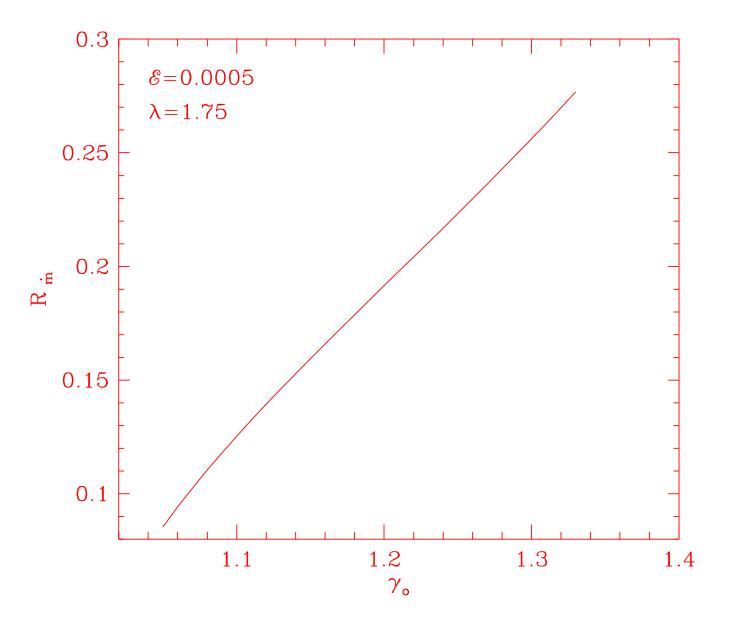
# Figure Captions

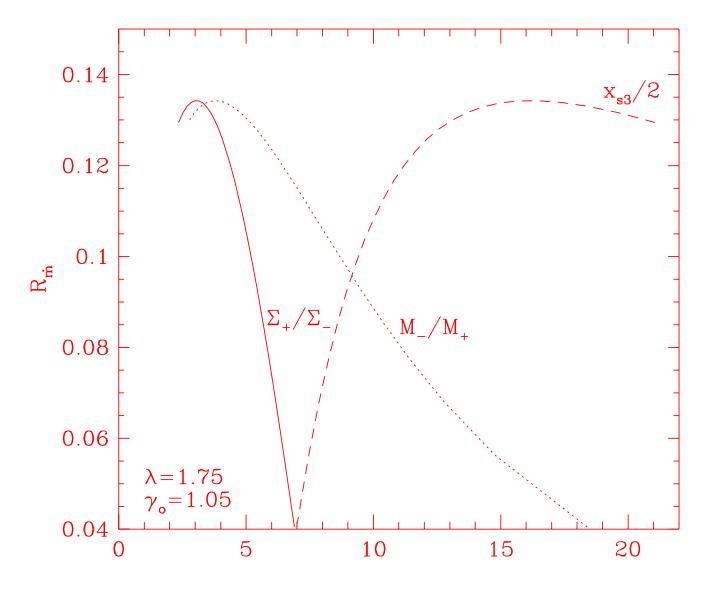
- Fig. 1: Few typical solutions which combine accretion and outflow. Input parameters are  $\mathcal{E} = 0.0005$ ,  $\lambda = 1.75$  and  $\gamma = 4/3$ . Solid curve with an incoming arrow represents the pre-shock region of the inflow and the dashed curve with an incoming arrow represents post-shock inflow which enters the black hole after passing through the inner sonic point (I). Dotted curves are the outflows for various  $\gamma_o$  (marked). Open circles are sonic points of the outflowing winds and the crossing point 'O' is the outer sonic point of the inflow. The leftmost shock transition  $(X_{s3})$  is obtained from unmodified Rankine-Hugoniot condition, while the other transitions are obtained when the mass-outflow is taken into account.
- Fig. 2: Ratio  $R_{\dot{m}}$  as outflowing polytropic index  $\gamma_o$  is varied. Only the range of  $\gamma_o$  for which the shock-solution is present is shown here. As  $\gamma_o$  is increased, the ratio is also increased. Since  $\gamma_o$  is generally anti-correlated with  $\dot{m}_{in}$ , this implies that  $R_{\dot{m}}$  is correlated with  $\dot{m}_{in}$ .
- Fig. 3: Variation of  $R_{\dot{m}}$  as a function of (a) shock-strength  $M_{-}/M_{+}$  (dotted) compression ratio  $\Sigma_{+}/\Sigma_{-}$  (solid) and the shock location  $X_{s3}$  (dashed) for  $\gamma_{o}=1.05$  and (b) specific energy  $\mathcal{E}$  for various  $\gamma_{o}$  (marked).  $\lambda=1.75$  throughout.
- Fig. 4:  $R_m$  as a function of the polytropic index  $\gamma$  of the inflow. The range of  $\gamma$  shown is the range for which shock forms in the flow. Suitably scaled density, velocity and area of the flow (at the base of the outflow) on the disk surface are also shown. See text for details. Non-monotonicity in  $R_m$  can be understood by the fact that the shock location, i.e., the area  $\mathcal{A}(r_{inj})$  and velocity  $\vartheta_{inj}$  of the outflow at the outflow origin go up with  $\gamma$ , but the density  $\rho_{inj}$  goes down.
- Fig. 5a: Few typical solutions for outflows forming out of an advective disk which does not include a standing shock wave. Incoming arrowed solid curve shows the inflow and the dashed arrowed curves with outgoing arrows show the outflows for  $\gamma_o = 1.3$  (top), 1.1 (middle) and 1.01 (bottom). At  $r_p$ , thermal pressure of the inflow is maximum.
- Fig. 5b: Variation of thermal pressure  $P_e$  of the incoming flow with radial distance. In a shock-free hydrodynamic flow, winds may form from the region around the pressure maximum.
- Fig. 6:  $R_{\dot{m}}$  as a function of outflowing polytropic index  $\gamma_o$  for various choices of the compression ratio  $R_{comp}$  of the outflowing gas at the pressure maximum. From bottom to top curve,  $R_{comp} = 2, 3, 4, 5, 6 \& 7$  respectively.
- Fig. 7: Variation of  $R_m$  (solid) as a function of the location  $r_p$  of the maximum pressure and the non-dimensional pressure (dotted)  $P_e(r_p)$  (multiplied by  $1.5 \times 10^{24}$  to bring to scale) are plotted.

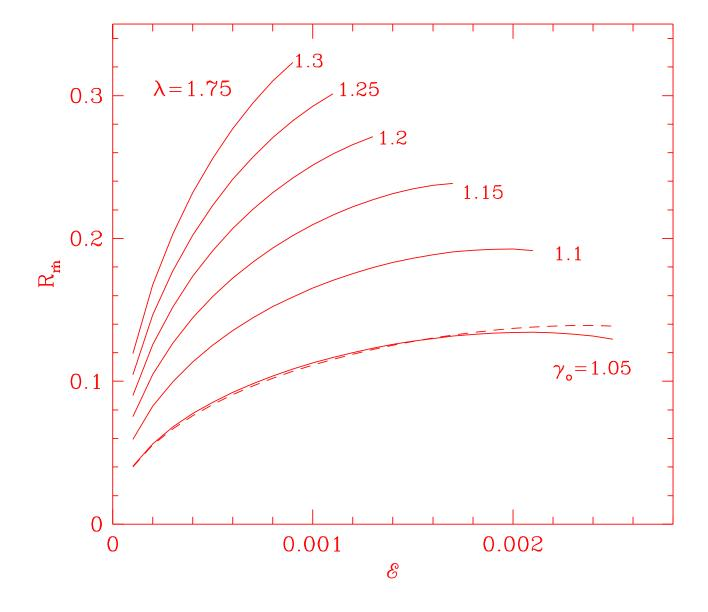
Fig. 8: Variation of effective proton (solid) and electron (dotted) temperatures in the advective regions of the accretion disk around a 10 solar mass black hole as functions of the accretion rates of the Keplerian flow. As Keplerian rate increases, both protons and elections cool down.

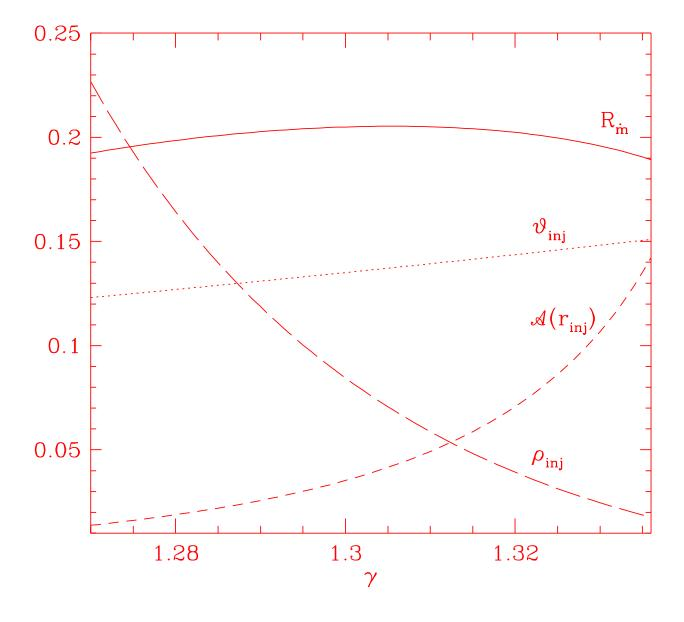
Fig. 9(a-b): (a) Variation of  $R_m$  as functions of the Eddington rate of the Keplerian component of the incoming flow for a range of the specific angular momentum. In the low luminosity objects the ratio is larger. (b)  $R_m$  as a function of the proton temperature  $T_p$  of the post-shock region. In (a),  $\lambda = 1.7$  (top curve),  $\lambda = 1.725$  (middle) and 1.75 (bottom curve). In (a) the angular momentum flux  $F(\lambda)$  of the outflow is also shown (dashed curve).

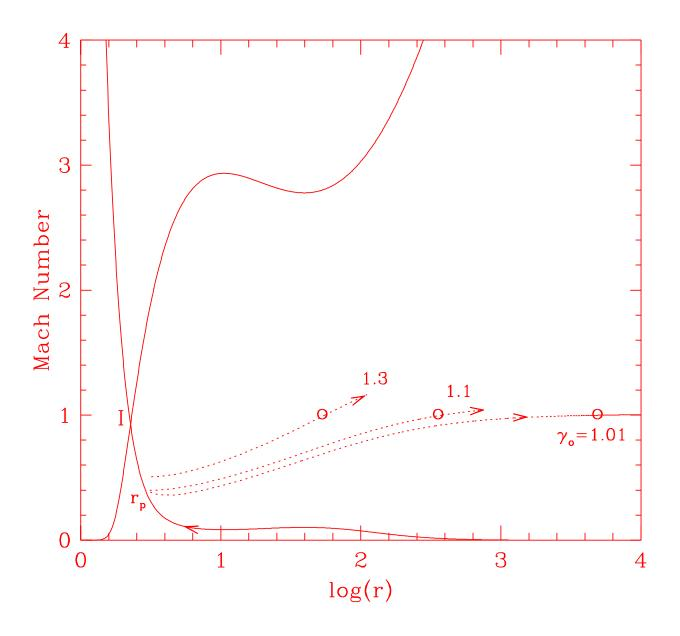


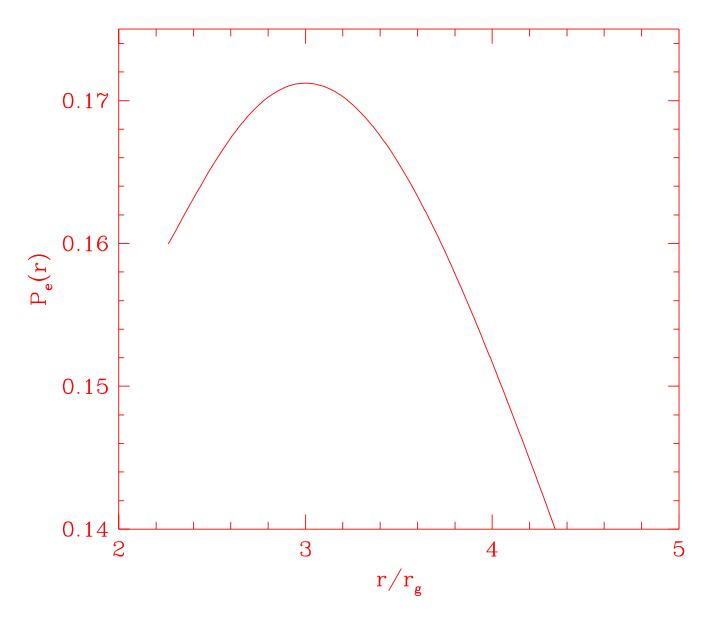












\_\_\_\_\_

